EPJ Web of Conferences **59**, 03004 (2013)
DOI: 10.1051/epjconf/20135903004

Systematic analysis of direct-drive baseline designs for shock ignition with the Laser MégaJoule

V. Brandon[1], B. Canaud[1,a], S. Laffite[1], M. Temporal[2] and R. Ramis[2]

[1] *CEA, DAM, DIF, 91297 Arpajon, France*
[2] *ETSIA, Universidad Politécnica de Madrid, Spain*

Abstract. We present direct-drive target design studies for the laser mégajoule using two distinct initial aspect ratios (A = 34 and A = 5). Laser pulse shapes are optimized by a random walk method and drive power variations are used to cover a wide variety of implosion velocities between 260 km/s and 365 km/s. For selected implosion velocities and for each initial aspect ratio, scaled-target families are built in order to find self-ignition threshold. High-gain shock ignition is also investigated in the context of Laser MégaJoule for marginally igniting targets below their own self-ignition threshold.

1. INTRODUCTION

Inertial confinement fusion (ICF) consists in illuminating a shell of fusible fuel with laser beams in direct-drive approach [1] or with x-ray in indirect drive approach [2]. Two laser facilities are built to achieve ICF with indirect drive configuration: the National Ignition Facility (NIF) in U.S.A. [3] and the Laser MégaJoule (LMJ) in France [4]. For LMJ, directly-driven self-ignition is possible [1] with indirect-drive beam geometry with zooming [5]. Moreover, Shock Ignition (SI) [6] and its application on LMJ [7] bring a new interest for direct-drive approach because it can offer high gain for non self-igniting target and allows to investigate the self-ignition threshold [8]. In this scheme, compression phase and ignition are separated. Usually, targets designs present high initial aspect ratio A, defined as the ratio of the deuterium-tritium (DT) ice-layer inner radius over the DT-ice layer thickness, around A = 7 for Fast-Ignition (FI) [9] or for Direct-Drive (DD) targets [1] and around A = 11 for indirect drive targets [4]. In our study, we explore low initial aspect ratios and moderate implosion velocities. Targets and laser pulses are optimized by a random-walk method and drive power variations in order to vary the implosion velocity. Then, selected target designs are scaled in Sec. 4 in order to scan the self-ignition threshold of transition between non- or marginally-igniting targets and burning targets, and finally shock ignition of marginally igniting targets at low implosion velocities is investigated.

2. DIRECT-DRIVE BASELINE DESIGNS

We set A = 3 and 5. Targets and laser pulses are described in Fig. 1. The initial aspect ratio considers only the 300 μg-DT ice-layer assuming that the polyimide (CH) ablator is fully expanded at the end of the laser pulse. CH ablator thickness and drive power are initially given by Rocket-effect formulae [2] for an implosion velocity of 310 km/s and assuming full ablation of CH. Calculations are then performed using the one-dimensional (1D) Lagrangian radiation-hydrodynamics code FCI1 [10]. Laser pulse shapes are initially defined to achieve implosion velocities around 310 km/s for each design and

[a] e-mail: benoit.canaud@cea.fr

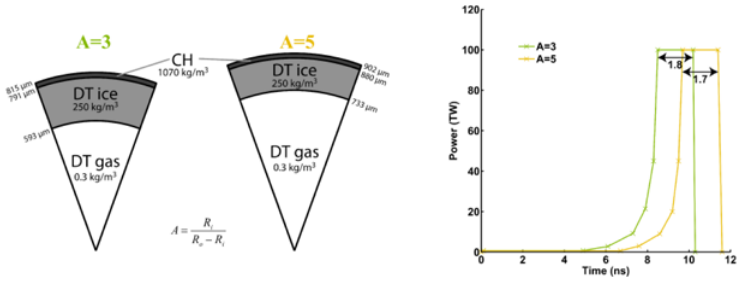

Figure 1. Targets designs (left) with A = 3 (left-green) and A = 5 (right-yellow) and laser pulses (right).

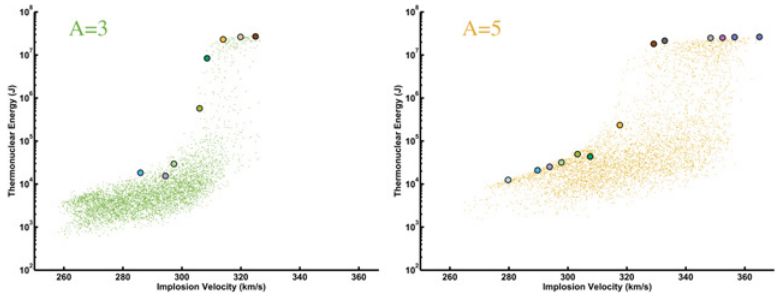

Figure 2. Thermonuclear energy versus implosion velocity for A = 3 (left) and A = 5 (right). Colored points are given in Table 1.

follow a Kidder-like law [11] to minimize entropy during the whole compression phase. The foot is chosen to get an inflight adiabat of one in the fuel layer. Drive duration is constant in our study and is sized to correspond to the ablator thickness with laser power drive of 100 TW. This first optimization is complemented by a random-walk method that consists in varying the pulse ramp in order to obtain a refined shock timing that maximizes the areal density at stagnation of non-igniting targets or the thermonuclear energy when target ignites. The drive power also varies. A new laser pulse is built for each random realization. Successive refinements of intervals are used to cover unexplored part of the parameter space and to get an optimum. The results are shown in Fig. 2 where thermonuclear energy is given versus implosion velocity for each aspect ratio. Each dot represents a 1D-implosion. Self ignition threshold is observed for an implosion velocity of 300 km/s for A = 3, and 325 km/s for A = 5. Thus, with the same fuel mass, the self-ignition kinetic-threshold is lower for A = 3 than for A = 5. We notice that the absorbed laser energy is higher for A = 3 than for A = 5 for the same implosion velocity. Thus the thermonuclear gain, above ignition, is roughly the same for both aspect ratios but not at the same implosion velocity (cf Table1).

3. SCALED TARGETS

We selected a few designs at the frontier of the data clouds for both A that are marked by colored points in Fig. 2. These points, summarized in Table 1, offer the maximum areal density (under self ignition threshold) or maximum thermonuclear energy (above self ignition threshold), with minimum absorbed energy for different implosion velocities. The average peak areal density is higher for A = 3 ($\rho r \simeq 19\,\mathrm{kg/m^2}$) than for A = 5 ($\rho r \simeq 16\,\mathrm{kg/cm^2}$). An Eulerian scaling [12] is applied to the previous set of designs that conserves velocities and laser intensities to explore thermonuclear energy as a

Table 1. List of working points selected to compute scaled targets.

A = 3				A = 5			
V (km/s)	E_a (kJ)	ρR (kg/m^2)	E_{th} (kJ)	V (km/s)	E_a (kJ)	ρR (kg/m^2)	E_{th} (kJ)
				280	171	1.46	12
286	215	18.5	18	**289**	181	15.0	21
294	233	18.8	15	**294**	187	15.3	25
297	238	18.4	29	**298**	193	15.6	32
306	234	18.6	573	**303**	199	15.8	49
308	250	18.7	8389	**308**	204	15.9	44
314	260	18.2	23032				
320	272	18.6	26216	**317**	219	16	234
325	283	18.9	26915	**329**	226	16	18 119
				333	233	16.4	21 411
				348	249	16.6	24 862
				352	264	16.4	25 064
				356	267	16.6	25 695
				365	280	16.7	26 296

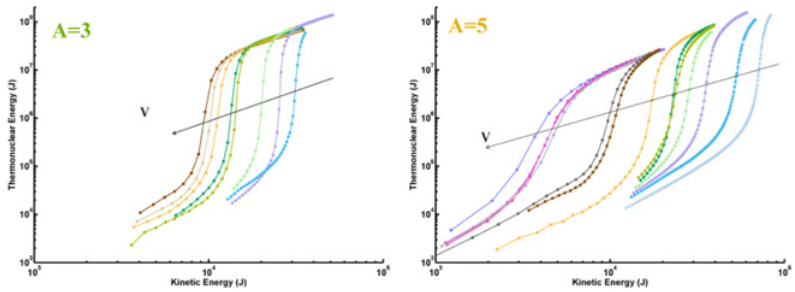

Figure 3. Thermonuclear energy as function of kinetic energy for A = 3 (left) and A = 5 (right). Each curve is scaled from a selected point described in Table 1.

function of kinetic energy (cf Fig. 3). Scaling laws are expressed in function of a scale factor f: $m_1/m_0 = f$, $E_1/E_0 = f$, $r_1/r_0 = f^{1/3}$, $t_1/t_0 = f^{1/3}$, $P_{laser\,1}/P_{laser\,0} = f^{2/3}$, $V_1/V_0 = 1$, $\rho_1/\rho_0 = 1$, and $I_1/I_0 = 1$. Self-ignition is always achieved for all curves with a kinetic self-ignition threshold which decreases with the implosion velocity. Such preliminary results are very promising and will be deeply detailed in a future article.

4. SHOCK IGNITION

The shock ignition scheme [6] consists in adding a high power spike at the end of the drive pulse. This spike creates a strong shock that propagates towards the hot spot which departs from an isobaric stagnation, and reduces the ignition threshold. Spike timing must be adjusted in function of the spike power as shown in Fig. 4. This approach is applied to a marginally-igniting target that is under its self-ignition threshold for A = 5 and $v = 317$ km/s (here, $f = 0.7$). Figure 4 represents the ignition window. Thermonuclear gain (∼90), defined as the ratio of thermonuclear energy over the absorbed energy, is exactly the same as the one obtained for the self-igniting target, when $f = 1$. Indeed, thermonuclear energy is roughly 17 MJ for 180 kJ of absorbed energy and a DT-mass of 210 μg.

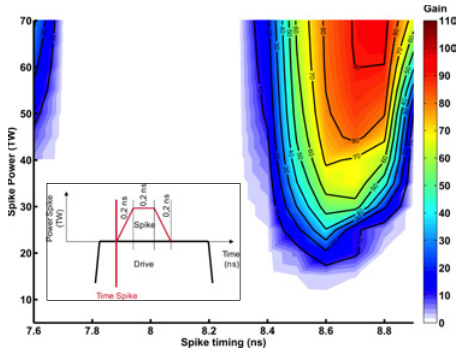

Figure 4. 1D gain versus spike power and time-of-launch for A = 5, f = 0.7, and V = 317 km/s.

5. CONCLUSION

We present preliminary results about two new families of target designs with initial aspect ratios A of 3 and 5. A large range of peak implosion velocities is explored by the means of a random walk method. Self-ignition is obtained at a higher implosion velocity for A = 5 than for A = 3. Selected points are identified that maximize thermonuclear energy and peak areal densities for given absorbed energies. Scaling laws that conserve implosion velocities are applied to this set of selected designs that allow to compose a large library of target designs in function of initial aspect ratio, peak implosion velocity, fuel mass and position relative to self-ignition threshold. Finally, shock ignition is considered for a reduced-size marginally-igniting target that produces a 1D gain of 93.

References

[1] B. Canaud, F. Garaude, C. Clique, N. Lecler, A. Masson, R. Quach and J. Van der Vliet, Nucl. Fusion **47**, 1652 (2007)
[2] J. D. Lindl, P. Amendt, R. L. Berger, S.G. Glendinning, S.H. Glenzer, S. W. Haan, L. Kauffman, L. Landen and L. J. Suter, Phys. Plasmas **11**, 339 (2004)
[3] E. I. Moses, Energy Conversion and Management **49**, 1795 (2008)
[4] J. Giorla, J. Bastian, C. Bayer, B. Canaud, M. Casanova, F. Chaland, C. Cherfils, C. Clique, E. Dattolo, P. Fremerye, D. Galmiche, F. Garaude, P. Gauthier, S. Laffite, N. Lecler, S. Liberatore, P. Loiseau, G. Malinie, L. Masse, A. Masson, M. C. Monteil, F. Poggi, R. Quach, F. Renaud, Y. Saillard, P. Seytor, M. Vandenboomgaerde, J. Van der Vliet and F. Wagon, Plasm. Phys. Control. Fusion **48**, B75 (2006)
[5] B. Canaud and F. Garaude, Nucl. Fusion **45**, L43 (2005)
[6] R. Betti, C. D. Zhou, K. S. Anderson, L. J. Perkins, W. Theobald and A. A. Solodov, Phys. Rev. Lett. **98**, 155001 (2007)
[7] B. Canaud, S. Laffite, V. Brandon, and M. Temporal, Las. Part. Beams **30**, 183 (2012)
[8] B. Canaud and M. Temporal, New J. Phys. **12**, 3037 (2010)
[9] S. Atzeni, A. Schiavi and C. Bellei, Phys. Plasmas **14**, 2702 (2007)
[10] E. Buresi, J. Coutant, R. Dautray, M. Decroisette, B. Duborgel, P. Guillaneux, J. Launspach, P. Nelson, C. Patou, J. M. Reisse and J. P. Watteau, Las. Part. Beams **4**, 531 (1986)
[11] R. E. Kidder, Nucl. Fusion **16**, 405 (1976)
[12] E. Falize, S. Bouquet and C. Michaut, Astrophys. Space Sci. **322**, 107 (2009)